Received: 21 May 2019 | Revised: 4 October 2019 | Accepted: 13 October 2019

DOI: 10.1002/jccs.201900200

JOURNAL OF THE CHINESE CHEMICAL SOCIETY

ARTICLE

Exploring beta amyloid cleavage enzyme-1 inhibition and neuroprotective role of benzimidazole analogues as anti-alzheimer agents

Archana S. Gurjar | **Vivek S. Solanki** | **Ankita R. Meshram** | **Suchita S. Vishwakarma**

Department of Pharmaceutical Chemistry, Principal K. M. Kundnani College of Pharmacy, Mumbai, India

Correspondence
Archana S. Gurjar, Department of Pharmaceutical Chemistry, Principal K. M. Kundnani College of Pharmacy, 23 Jote Joy, R. S. Marg, Cuffe Parade, Mumbai 400 005, India.
Email: gurjaras@gmail.com

Funding information
University of Mumbai, Grant/Award Numbers: Minor Research Project Grant 509, APD/ICD/2018-19

Abstract

Beta amyloid cleavage enzyme-1 (BACE1) is the key enzyme involved in Aβ peptide formation in Alzheimer's disease pathogenesis. We intend to target this enzyme by exploring benzimidazole analogues against BACE1 as potential anti-Alzheimer agents. Docking studies were performed to determine the hydrogen bond interactions between the designed molecules and the target protein's active site. Research indicates the relationship between oxidative stress and Aβ effect in precipitating neurodegeneration; hence, the series was also studied *in vitro* to ascertain its neuroprotective role by performing the lipid peroxidation assay. *In silico* absorption, distribution, metabolism, and excretion studies were undertaken to assess the drug-like suitability of the analogues. To judge the effect of the synthesized analogues on central nervous system (CNS), toxicity and memory model studies were conducted on mice. Thus, overall results showcase analogues **11** and **14** as the most promising ones with the dual role of BACE1 inhibition and neuroprotection, along with memory retention.

KEYWORDS

BACE1, docking, in silico ADME studies, in vitro LPO assay, memory model studies, toxicity study

1 | INTRODUCTION

Alzheimer's disease (AD) is an advancing multifaceted neurodegenerative disorder resulting in the loss of the neurons and intellectual abilities including memory and reasoning, which imposes tremendous emotional, social, and economic burden on the patient, his or her family, and the community.[1,2] Several hypotheses have been proposed to be involved in the etiopathogenesis of AD such as beta amyloid (Aβ) formation and its accumulation, Tau (τ) hyperphosphorylation and aggregation, neurotransmitter imbalance, oxidative stress, and others including calcium dysregulation and inflammation.[3] Amongst the etiological factors, beta amyloid cleavage enzyme-1 (BACE1, beta-secretase) is the key enzyme responsible for the formation of Aβ peptides. BACE1 is a type I transmembrane enzyme with high concentration in neurons and belongs to the same retroviral and pepsin aspartic protease family. It has an optimum acidic pH with the correct sequence specificity for the processing of amyloid precursor protein (APP), leading to an increased Aβ generation.[4,5] It regulates a range of neuronal

functions and the formation of a myelin sheath in peripheral nerve cells. BACE1 knockout mice do not produce Aβ from APP in the brain but are viable, suggesting that targeted inhibition of the BACE1 enzyme would considerably reduce the on-target toxicities.[6] The BACE1 crystal structures project the active site as a long cleft with two catalytic aspartate residues (Asp32 and Asp228) for substrate recognition.[7,8] Beta-secretase inhibitors broadly belong to two categories: peptidomimetic and nonpeptidic. The nonpeptide BACE1 inhibitors can cross the blood–brain barrier and reach the target site more easily compared to the peptidomimetic ones. Some of the nonpeptide inhibitors reported in literature are: LY2811376 [(S)-4-(2,4-difluoro-5-pyrimidin-5-yl-phenyl)-4-methyl-5,6-dihydro-4H-[1,3]thiazin-2-ylamine],[9] Lanabecestat (AZD3293), biflavonoids (2,3-dihydroamentoflavone and 2,3- dihydro-6-methylginkgetin),[10] and various nonpeptidic scaffolds such as amidino- or guanidino-heterocycles, which were found to be apt BACE1 inhibitors due to hydrogen bond formation with the catalytic aspartyl dyad.[11]

Research depicts that the Cu^{2+} ion may induce the conversion of normal Aβ42 to abnormal conformation, in turn facilitating its aggregation into fibril. There exists an involvement of metal ions in the formation of amyloid fibrils, and this metallo-Aβ complex leads to oxidative stress in the brains of AD patients.[12,13] Aβ-mediated neurotoxicity is a result of the intracellular accumulation of reactive oxygen species, leading to lipid oxidation. Oxidative stress and Aβ accumulation leads to the formation of lipid peroxidation (LPO) product; hence, antioxidant activity estimation would be beneficial to assessing the neuroprotective role.[14,15]

Nitrogen-containing heteroaromatics are crucial core scaffolds used to design drugs and represent one of the most biologically active class of compounds. Investigation of the reported benzimidazole analogues showed a wide range of pharmacological activities, such as antimicrobial, analgesic, anticonvulsant, antihypertensive, anticancer, antitumor, and antiviral.[16] Malamas (**1**) and Gravenfors (**2**) et al have independently reported amino imidazoles as potent BACE1 inhibitors (Figure 1).[17,18] Benzimidazole derivatives fused with the oxadiazole ring system exhibited moderate antioxidant activity.[19] Conventional methods for the synthesis of benzimidazoles make use of harsh strong acids or mineral acids for the reaction of o-aryldiamines with carboxylic acids and their derivatives.[20] Other methods have reported the direct condensation of o-aryldiamines and aldehydes in the presence of various reagents or catalysts such as dioxane,[21] copper hydroxide,[22] NH_4Cl,[23] $MgCl_2.6H_2O$,[24] H_2O_2 and HCl,[25] boric acid,[26] lanthanum chloride,[27] and triflates.[20,28] Some of the reagents

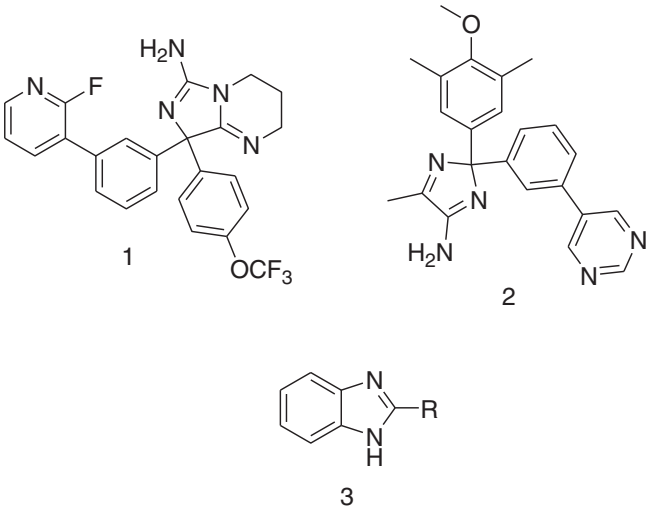

FIGURE 1 Aminoimidazole and benzimidazole scaffolds

are carcinogenic, such as dioxane; costly (lanthanum triflates); or unstable. A search of suitable reagents led to ceric ammonium nitrate (CAN), an inexpensive, easily available oxidizing agent for many functional groups (alcohols, phenols, and ethers), as well as C—H bonds, especially the benzylic ones. Aqueous CAN in catalytic amounts can be used for the efficient synthesis of heterocycles.[29]

On the basis of the above literature review, 1H-benzo[d] imidazole scaffold (**3**) has been explored, and the designed series of benzimidazole analogues has been targeted for the dual role of BACE1 inhibition and antioxidant activity (Table 1). Based on molecular docking and *in silico* absorption, distribution, metabolism, and excretion (ADME) studies, analogues that exhibited better interactions and drug-like properties were selected for the synthesis and pharmacological evaluation, which comprises *in vitro* LPO assay, acute toxicity studies, and memory model studies.

2 | RESULTS AND DISCUSSION

2.1 | Molecular docking

Molecular docking is a valuable tool to anticipate ligand–enzyme interactions. A literature survey indicates the role of the two catalytic aspartyl BACE1 active site residues (Asp32 and Asp228) in enzymatic catalysis.[30] The X-ray crystal structure of BACE1 complexed with octapeptide inhibitor OM00-3 (PDB: 1m4h) projected eight subsites that can be associated during ligand–enzyme interactions.[31]

The PDB 1m4h structure showcased a good activity profile with K_i 0.3 nM and was thus considered for the docking studies.[31] The docking protocol was validated with an root mean square deviation of 1.51 (Figure 2). The octapeptide inhibitor OM00-3 occupied S_1, S_2, S_1', and S_2' sub sites and interacted primarily with the catalytic

TABLE 1 *In silico* ADME results of 2-substituted-1H-benzo[d]imidazole analogues

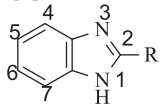

No.	R	Mol. wt.[a]	Donor HB	AccptHB	QPlogP o/w	QP logBB	QPPMDCK	Rule of five	% human oral absorption
4	H	118.14	1	2	1.32	0.10	1,402.18	0	95.86
5	CH_3	132.17	1	2	1.52	0.18	1868.13	0	100
6	CH_2CH_3	146.19	1	2	2.55	0.17	2,247.21	0	100
7	$CH(CH_3)_2$	160.22	1	2	2.62	0.21	2,588.39	0	100
8	CH_2Cl	166.61	1	2	2.46	0.38	5,166.26	0	100
9	Ph	194.24	1	2	3.26	0.28	2,698.87	0	100
10		184.20	1	2	2.57	0.23	2,233.4	0	100
11		239.23	1	3	2.62	−0.54	365.19	0	93.81
12	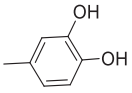	226.23	3	3	1.72	−0.74	247.49	0	85.70
13	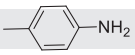	209.25	3	3	2.21	−0.33	628.52	0	95.32
14	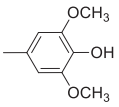	270.29	2	4	2.81	−0.27	1,130.27	0	100
15		239.23	1	3	2.53	−0.66	272.58	0	91.14
16	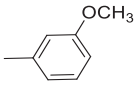	224.26	1	2	3.34	0.21	2,702.77	0	100
17		210.24	2	2	2.52	−0.13	1,052	0	100
18	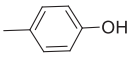	210.24	2	2	2.42	−0.27	742.27	0	100
19	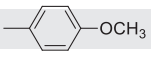	224.26	1	2	3.34	0.21	2,696.25	0	100
20	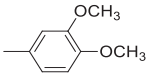	254.29	1	3	3.5	0.14	2,695.2	0	100
21	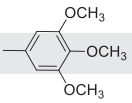	284.31	1	4	3.58	0.08	2,695.96	0	100
22	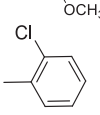	228.68	1	2	3.62	0.39	5,347.96	0	100
23	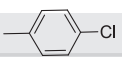	228.68	1	2	3.68	0.45	6,664.27	0	100

[a]g/mol.

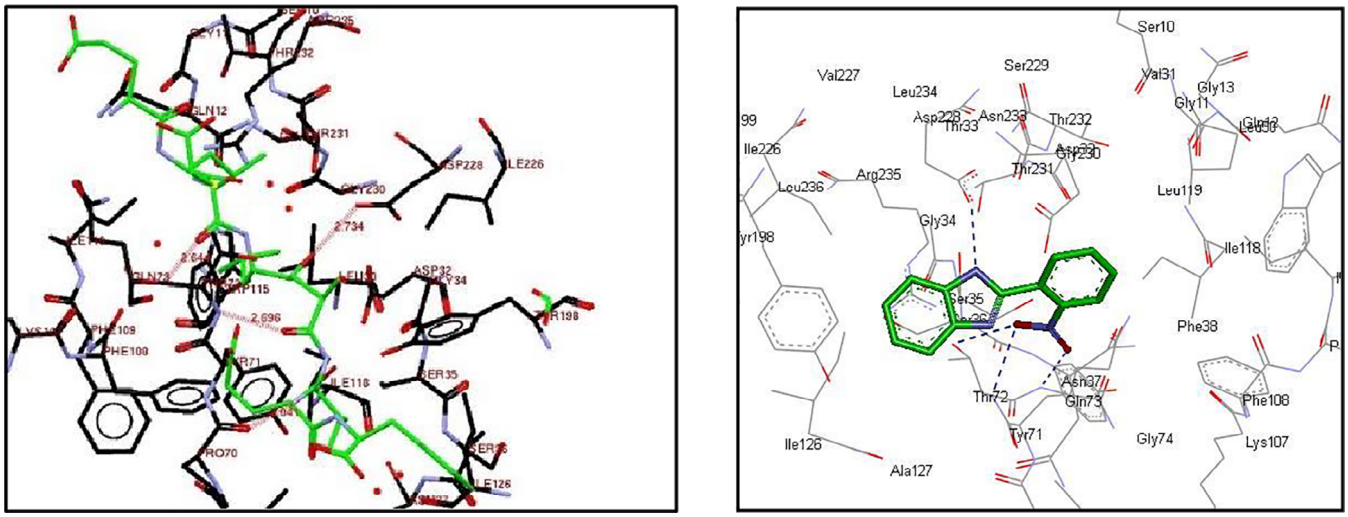

FIGURE 2 Docking pose of OM00-3 and analogue 11 in BACE1 active site

aspartate dyad, Asp32 and/or Asp228, which plays a crucial role in enzymatic catalysis and inhibitor binding. The amino acid residues of various subsites are as follows: S_1: Leu30, Asp32, Tyr71, Gln73, Phe108, Asp228, Gly230; S_2: Tyr71, Thr72, Gln73, Gly230, Thr231, Arg235; S_1': Gly34, Tyr71, Thr72, Asp228; and S_2': Gly34, Ser35, Val69, Pro70, Tyr71, Tyr198.[31]

In the present study, a series was designed using 1H-benzo[d]imidazole scaffold with various substituents at 2-position in the imidazolyl ring. (Table 1) The substituents have been varied from simple alkyl groups such as methyl and ethyl to phenyl and heteroaryl. Furthermore, mono-, di-, and trisubstitutions with different functional groups have been tried at various positions in the phenyl ring. In the designed series, most of the analogues have interacted with BACE1 active site residues. The analogues mainly occupied S_1 and S_1' subsites, analogues **5**, **8**, **9**, **18**, and **19** have occupied the S_2 subsite probably due to interaction with Arg235 residue of the BACE1 active site. Some analogues, that is, **11**, **12**, **13**, and **14**, interacted well with the catalytic aspartate dyad. Amongst them, substituents such as amino, hydroxy, and methoxy groups formed H-bonds with the active site residues, while nitro-substituted analogue interacted through the NH of benzimidazole ring. Thus, these benzimidazole analogues might be promising candidates for AD.

2.2 | *In silico* ADME studies

The drug-like properties of the analogues were assessed by performing *in silico* ADME studies. The *in silico* ADME study results were found to be very much within the QikProp recommended ranges (Table 1).[32,33] The molecular weight (Mol. wt.) in the series varied from 118 to 284 with an outlier analogue **4**. The number of donor hydrogen bonds (DonorHB) were found to be 1–3, while acceptor hydrogen bonds (accptHB) were 2–4. The QPlogPo/w parameter is an important factor for partitioning of drugs between lipophilic and hydrophilic phases. The QPlogPo/w values were favorable as observed, 1.32–3.68. Similarly, the QPlogBB values for all the analogues were obtained in a small range of −0.74 to 0.39. The QPPMDCK model modestly mimics the blood–brain barrier. The QPPMDCK values were gauged as optimum to great. None of these analogues violated Lipinski's rule of five for drug-like properties. The percentage of human oral absorption was found to be high, that is, more than 85%, for all the analogues. Thus, these analogues can be presumed to be potential drug candidates with desirable pharmacokinetic properties.

2.3 | Synthesis and characterization

On the basis of computational results, designed analogues were chosen for the synthesis using a CAN reagent and further characterized with infrared (IR), nuclear magnetic resonance (NMR), and mass spectroscopy. The synthesized analogues IR spectra portrayed absorption bands nearly identical to the literature for the functional group present in them. ^{1}HNMR and ^{13}CNMR spectra exhibited predictable delta values for the protons and carbon atoms, respectively.[34] Mass analysis of the analogues showed the expected molecular mass values. Thus, all the results of identification and characterization optimistically confirms the formation of synthesized analogues and the correctness of their anticipated structure. The spectra have been provided in the Supplementary Information.

2.4 | Pharmacological evaluation

2.4.1 | *In vitro* LPO assay

As discussed earlier, oxidative stress and Aβ accumulation leads to the formation of LPO product, so antioxidant activity was determined by means of *in vitro* LPO assay to portray the neuroprotective role exhibited by the analogues. The IC_{50} value of the reference compound ascorbic acid was observed to be 47.77 μM and in the range of 25–265 μM for the benzimidazole analogues (Table 2). Amongst them, two analogues (**11** and **14**) exhibited IC_{50} values of 25.68 and 53.82 μM, better than others in the series. The *in vitro* LPO assay results for analogue **16** were incoherent and were therefore not considered. Thus, the *in vitro* LPO assay results for these analogues showcased their neuroprotective role.

2.4.2 | Correlation of docking and LPO assay results

The docking results of benzimidazole analogues **11**, **13**, and **14** correlated with the *in vitro* antioxidant activity results. These analogues exhibited interactions with the catalytic dyad, which plays a vital role in inhibitor binding and enzymatic catalysis. Analogously, these compounds exhibited better IC_{50} values in the *in vitro* LPO assay.

2.4.3 | Acute toxicity studies

Based on the above correlation from the three analogues, **11** and **14** with good LPO assay IC_{50} values were selected for the *in vivo* studies. Following the guidelines, an acute toxicity study of representative benzimidazole analogue **11** led to identification of a safe and nonlethal dose of 1,000 mg/kg in Swiss albino mice.

TABLE 2 *In vitro* LPO assay results

Analogue no.	IC_{50} (μM)[a]
4	127.12
9	84.18
11	25.68
12	127.37
13	69.50
14	53.82
15	265.08
17	81.41
Ascorbic acid	47.77

[a]Values are the average of three experiments.

2.5 | Memory model studies

2.5.1 | Elevated plus maze model

This model was used to judge the effect of the synthesized compounds on the memory and learning of Swiss albino mice. Individual groups consisting of six mice (three male and three female) were treated with analogue **11** at a dose of 50 and 100 mg/kg and analogue **14** at a dose of 50 mg/kg (Table 3). There was substantial decrease in the transfer latency (TL) compared to the toxicant group. The results demonstrate successful retention of memory in the mice by both these analogues. However, TL recorded for analogue **11** at 100 mg/kg dose level was more effective.

2.5.2 | Passive avoidance test

The test was conducted after 24 hr (on ninth day) without shock, and the time required to step down on the grid floor from the wooden box was recorded as step-down latency (SDL), a measure of learning. On comparison with the toxicant, analogues **11** and **14** retained memory as the respective dosed animals took prolonged time to step down from the block. Furthermore, relating the two test compounds, analogue **11** showcased better results, analogous to the elevated plus maze (EPM) results (Figure 3).

Data for the above two tests were analyzed by one-way analysis of variance. A significant statistical difference was found between control and test groups (p value > .01). Hence, post-test was applied to the data using Dunnett multiple comparison tests. According to Dunnett test, if q is greater than 2.730, then p value is less than .05.

3 | EXPERIMENTAL

3.1 | Structure-based drug design and molecular docking

For ligand and protein preparation, Sybyl version 8.1.1 and Biopolymer module (Tripos International, St Louis, MO) running on Red Hat Enterprise Linux (RHEL) workstation were used, respectively.[35] GOLD version 5.2.2 (CCDC Ltd., England, UK) was used for docking studies.[36]

3.2 | Ligand and protein preparation

All the ligands and protein were prepared as indicated in our earlier published article.[37]

TABLE 3 Effect of test compounds on transfer latency in elevated plus-maze model

S. No.	Groups	Mean transfer latency ± *SD* in s
1	Control	31.600 ± 3.209
2	Standard (piracetam 200 mg/kg)	21.600 ± 2.302
3	Toxicant (scopolamine HBr: 0.4 mg/kg)	80.200 ± 5.070
4	Analogue **11** (50 mg/kg)	59.400 ± 2.302
5	Analogue **11** (100 mg/kg)	46.600 ± 2.966
6	Analogue **14** (50 mg/kg)	66.000 ± 3.873

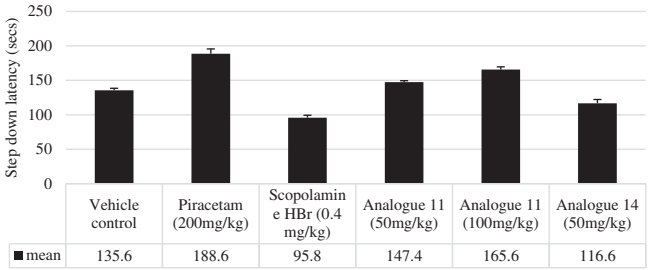

FIGURE 3 Passive avoidance test results

3.3 | Molecular docking

The same steps were followed to prepare and validate the docking protocol as mentioned in our previous article.[37]

3.4 | *In silico* ADME studies

In silico ADME studies were carried out on the RHEL workstation with QikProp software version 3.3 (Schrodinger LLC, New York, NY).[38]

3.5 | Method

LigPrep was used to preprocess the structures for input to QikProp for in silico ADME prediction. The structures were optimized by means of the OPLS-2005 force field. The results can be viewed in the generated-OUT file.

3.6 | Synthesis and characterization

All materials used were acquired from commercial sources. The purity of starting materials was assessed by thin-layer chromatography (TLC), as well as by determination of their physical constants. Reactions were routinely monitored by thin-layer chromatography on Merck silica gel F_{254} plates, and spots were visualized under an ultraviolet lamp at 254 nm. Analab melting point apparatus μThermoCal10 was used to determine the physical constants, and a Shimadzu IR Affinity-1 fourier transform infra red (FTIR) spectrophotometer was used to record IR spectra. ^{1}HNMR spectra were registered in parts per million (ppm) with tetramethyl silane as an internal standard on Mercury Plus 300 MHz (Varian) and Bruker 300 Ultra shield NMR Spectrometer by using acetone/ dimethyl sulfoxide (DMSO) solvent. Bruker BioSpin GmbH at 100 MHz was utilized for ^{13}CNMR in DMSO. The spectrometer used for recording the mass spectra was 410 Prostar Binary LC with 500 MS IT PDA detectors (Varian Inc).

3.7 | Method

3.7.1 | Synthesis of 1H-benzo[d] imidazole (1)

The synthesis was carried out as per the standard reference procedure, and the reactions were monitored using an n-hexane: ethyl acetate (1:1) TLC system.[39]

3.7.2 | Synthesis of substituted-2-phenyl-1H-benzo[d]imidazole analogues (9, 11, 12, 14–17)

A total of 0.5 g. o-phenylenediamine (4.629 mmol) and substituted aromatic aldehydes (4.629 mmol) were stirred in 15 ml ethanol in the presence of cerric ammonium nitrate (0.1 mmol) for 48 hr. The reaction was monitored by TLC technique using ethyl acetate: n-hexane (1:1). The reaction mixture was then poured in brine solution for precipitation. The precipitate was then filtered, washed with cold water, dried using vacuum, and recrystallized with ethanol: water (1:1) mixture to obtain the title compounds. The synthesized compounds purity was confirmed by TLC, IR, ^{1}HNMR, ^{13}CNMR, and mass spectroscopy.

3.7.3 | Synthesis of 2-(4-aminophenyl)-1H benzo[d]imidazole (13)

A total of 1.9 g. of o-phenylenediamine (17.592 mmol) and 2.25 g. of p-aminobenzoic acid (16.423 mmol) were refluxed for 2 hr in the presence of o-phosphoric acid. The cooled reaction mixture was then poured on crushed ice with stirring. The pH of the solution was adjusted to 7 using 5 M sodium hydroxide solution.[40] The brown

color precipitate was filtered, dried, and recrystallized from methanol. The purity of the compound was checked by TLC and confirmed by IR, ^{1}HNMR, ^{13}CNMR and mass. TLC system used was n-hexane: ethyl acetate (1:1).

3.8 | Spectral and analytical data

3.8.1 | 1H-benzo[d]imidazole (4)

Buff white (s), Melting point—172°C, Yield—78%, R_f—0.157, 0.162, FTIR (cm^{-1}): 3,064.06 (NH), 2,794.97 (C—H), 1,246.07 (C—N), 1,587.48 (C═N), 1,409.06 (C═C), ^{13}CNMR (ppm, 100 MHz, DMSO-d_6): δ 141.86, 121.51, 118.91, 111.57. MS: (M+1): 119.2 (Figures S1 and S2).

3.8.2 | 2-phenyl-1H-benzo[d] imidazole (9)

Pale yellow (s), Melting point—288°C, Yield—79%, R_f—0.157, 0.162, FTIR (cm^{-1}): 3,220 (NH), 3,118.90 (C—H), 1,315.45 (C—N), 1,540 (C═N), 1,436.97 (C═C), ^{1}HNMR (ppm, 300 MHz, DMSO-d_6): δ 11.914 (s, 1H), 7.235–7.252 (t, J = 2.55 Hz), 7.710–7.725 (t, J = 2.25 Hz), 8.252–8.268 (d, J = 4.8 Hz), 7.523–7.588 (m, J = 9.45 Hz). ^{13}CNMR (ppm, 100 MHz, DMSO-d_6): δ 150.37, 130.86, 129.08, 128.81, 126.96, 126.12, 123.22, 114.72. MS: (M+1): 195.2 (Figures S3, S4, S5, and S6).

3.8.3 | 2-(2-nitrophenyl)-1H-benzo[d] imidazole (11)

Brown (s), Melting point—270°C, Yield—91.6%, R_f—0.512, 0.3928, FTIR (cm^{-1}): 3,153.61(NH), 3,072.60 (C—H), 1,246.02 (C—N), 1,541.12, 1,307.74 (NO_2), 1,651.07 (C═N), 1,436.97 (C═C), ^{1}HNMR (ppm, 300 MHz, DMSO-d_6): δ 13.051(s, 1H), 7.560–7.585 (d, J = 7.5 Hz), 7.216–7.280 (t, J = 9.6 Hz), 7.839–7.893 (td, J = 9.6 Hz), 7.649–7.673 (d, J = 7.2 Hz), 7.649–7.673 (dd, J = 1.35 Hz), 8.015–8.045 (dd, J = 1.2 Hz), 7.963–7.999 (dd, J = 1.35 Hz), 7.728–7.733 (d, J = 1.5 Hz). ^{13}CNMR (ppm, 100 MHz, DMSO-d_6): δ 148.92, 147.26, 132.58, 130.88, 130.83, 124.24, 123.02, 121.83, 119.20, 111.61. MS: (M+2): 241.2 (Figures S7, S8, and S9).

3.8.4 | 2-(3, 4-dihydroxyphenyl)-1H-benzo[d]imidazole (12)

Pale yellow (s), Melting point—236°C, Yield-66.66%, R_f—0.081, 0.085, FTIR (cm^{-1}): 3,379.43 (OH), 3,100 (NH), 2,924.21 (C—H), 1,280.79 (C—N), 1,605.81 (C═N), 1,450.53 (C═C). ^{1}HNMR: (ppm, 300 MHz, DMSO-d_6), δ 12.576(s, 1H), 6.832–6.859 (d, J = 8.1 Hz), 6.637–6.663 (d, J = 7.8 Hz), 7.635–7.657 (d, J = 6.6 Hz), 7.469–7.444 (d, J = 7.5 Hz), 6.984–7.011 (d, J = 8.1 Hz), 8.893 (s, OH). ^{13}CNMR (ppm, 100 MHz, DMSO-d_6): δ 147.13, 145.43, 145.36, 144.57, 142.66, 135.89, 127.73, (121.96, 121.76-d), 120.33, 118.72, (117.08, 116.62-d), (115.69, 115.55-d), 113.44. MS: (M+2): 228.3 (Figures S10, S11, and S12).

3.8.5 | 2-(4-aminophenyl)-1H-benzo[d] imidazole (13)

Buff white (s), Melting point—245°C. Yield—51%, R_f—0.264, 0.230, FTIR (cm^{-1}): 3,350 (NH), 3,439.23 (NH_2), 2,977.26 (C—H), 1,273.07 (C—N), 1,608.70 (C═N), 1,444.75 (C═C). ^{1}HNMR: (ppm, 300 MHz, DMSO-d_6), δ 11.676 (s, 1H), 7.494–7.523 (dd, J = 3.0 Hz), 7.117–7.159 (dd, J = 3.0 Hz), 7.948–8.008 (dd, J = 4.65 Hz), 6.773–6.841 (dd, J = 2.04 Hz), 5.123 (s, NH_2). ^{13}CNMR (ppm, 100 MHz, DMSO-d_6): δ 152.52, 150.50, 127.68, (121.28, 120.99-d), 117.88, 117.28, 113.48, 110.51. MS: (M+1): 210.2 (Figures S13, S14, and S15).

3.8.6 | 2-(4-hydroxy-3,5-dimethoxyphenyl)-1H-benzo[d] imidazole (14)

Brown (s), Melting point—177°C, Yield—78%, R_f—0.230, 0.264, FTIR (cm^{-1}): 3,345.67 (OH), 3,201.97 (NH), 2,970 (C—H), 1,275.90 (C—N), 1,218.10, 1,112.01 (C—O—C), 1,602.91 (C═N), 1,465.96 (C═C). ^{1}HNMR: (ppm, 300 MHz, DMSO-d_6), δ 12.691 (s, 1H), 7.485–7.515 (t, J = 4.5 Hz), 7.158–7.188 (dd, J = 2.85 Hz), 7.599–7.627 (s, 1H), 6.989 (s, 1H), 6.344 (s, 1H), 8.902 (s, 1H), 3.884 (s, 1H). ^{13}CNMR (ppm, 100 MHz, DMSO-d_6): δ 148.14, 143.83, 134.91, (122.27, 121.93-d), 121.34, (118.86, 118.30-d), 110.82, 106.69, 104.11. MS: (M+2): 272.2 (Figures S16, S17, and S18).

3.8.7 | 2-(3-nitrophenyl)-1H-benzo[d] imidazole (15)

Light brown (s), Melting point—205°C, Yield—73.2%, R_f—0.710, 0.6, FTIR (cm^{-1}): 3,286.70 (NH), 3,086.11 (C—H), 1,292.31 (C—N), 1,550.71, 1,550.71 (NO_2), 1,643.35 (C═N), 1,643.35(C═C). ^{1}HNMR: (ppm, 300 MHz, DMSO-d_6), δ 13.295 (s, 1H), 7.589–7.709 (d, J = 4.8 Hz), 7.250–7.266 (d, J = 4.8 Hz), 9.012–9.024

(t, J = 1.8 Hz), 9.012–9.024 (dt, J = 3.2 Hz), 7.83–7.88 (3s, 1H), 8.312–8.350 (2 dd, J = 1.05 Hz, 0.75 Hz). ^{13}CNMR (ppm, 100 MHz, DMSO-d_6): δ 149.02, 148.35, 135.25, 132.45, 131.71, 130.66, (124.46, 124.17-d), (122.80, 122.54-d), (121.56, 121.54-d), (121.25, 120.79-d), 117.32. MS: (M+2): 241.2 (Figures S19, S20, and S21).

3.8.8 | 2-(3-methoxyphenyl)-1H-benzo[d] imidazole (16)

Dark brown (s), Melting point—204°C, Yield—67.17%, R_f—0.756, 0.8, FTIR (cm^{-1}): 3,097.68 (NH), 2,985.81 (C—H), 1,271.09 (C—N), 1,238.30, 1,010 (C—O—C), 1,620.21 (C═N), 1,462.04 (C═C). ^{1}HNMR: (ppm, 300 MHz, DMSO-d_6), δ 12.93 (s, 1H), 7.462–7.489 (d, J = 8.1 Hz), 7.043–7.055 (t, J = 4.05 Hz), 7.749–7.760 (t, J = 1.65 Hz), 7.238–7.434 (d, J = 1.65 Hz), 7.772–7.776 (d, J = 1.2 Hz), 7.577–7.618 (dd, J = 3.3 Hz), 7.194–7.225 (dd, J = 3.0 Hz), 7.070–7.082 (dd, J = 0.9 Hz), 3.865 (s, 3H) (Figures S22 and S23).

3.8.9 | 2-(2-hydroxyphenyl)-1H-benzo[d] imidazole (17)

Pale yellow (s), Melting point—237°C, Yield—74%, R_f—0.842, 0.88, FTIR (cm^{-1}): 3,326.39 (OH), 3,057.30 (NH), 2,924.21 (C—H), 1,261.50 (C—N), 1,591.34 (C═N), 1,454.39 (C═C). ^{13}CNMR (ppm, 100 MHz, DMSO-d_6): δ 157.97, 131.68, 131.33, 130.17, 126.66, 126.16, (122.58, 122.50-d), 119.06, 117.13, 115.01, 112.54, 110.78. MS: (M +1): 211.2 (Figures S24 and S25).

3.9 | Pharmacological evaluation

3.9.1 | *In vitro* LPO assay

Commercial-grade chemicals and solvents were purchased. Remi centrifuge (R-4C DX) was used for centrifugation of the solutions. Absorbance was recorded on Thermo scientific ultraviolet visible spectrophotometer (Thermosci. Evolution 300).

3.10 | Method

A 0.1 ml test sample, 0.2 ml brain tissue homogenate, and 0.2 ml of 8.1% sodium dodecyl sulfate were mixed together. Furthermore, 1.5 ml of 20% acetic acid and 1.5 ml of 8% 2-thiobarbituric acid (TBA) were added to the above mixture, and its final volume was adjusted to 4 ml with distilled water. This solution was heated in a water bath for 60 min at 95°C. Then, the solution was cooled to room temperature, and the final volume was again increased to 5 ml with distilled water. For extraction purposes, 5 ml mixture of n-butanol: pyridine (15:1) was utilized. After centrifugation at 4,000 rpm for 10 min, the upper organic solution's optical density was noted at 532 nm against an appropriate blank.[41] The reference standard and all analogues were assayed by the same method. The following formula was used for calculating the percentage inhibition, that is, decrease in TBA reacting substance formation against an appropriate control.

$$\text{Percentage inhibition} = \left(\text{Abs}_{\text{control}} - \text{Abs}_{\text{sample}}\right) \times 100/\text{Abs}_{\text{control}}.$$

IC_{50} values were calculated from an average of triplicate analysis.

3.11 | Acute toxicity studies

3.11.1 | Animals

Swiss albino mice weighing 20–25 g of male and female genders were procured from the registered breeder Bombay Veterinary College (BVC), Mumbai. The animals were maintained in hygienic condition in the animal house in group of six in clean protected plastic mice cages containing husk bedding. The animals were fed standard pellet food and aqua distil water. Animal house environmental conditions were maintained between 22 ± 2°C with 60 ± 10% relative humidity in a 12-hr light and 12-hr dark cycle. In order to acclimatize, prior to the experimental studies, the animals were housed for 15 days (protocol number: KMKCI/IAEC/08/2017).

3.12 | Method

An acute toxicity study was performed on two male and two female albino mice at an initial dose of 1,000 mg/kg p.o to study morbidity and mortality, if any, as per OECD-423 guidelines.[42,43]The aqueous suspension of test compound in 1% wt/vol sodium carboxymethylcellulose was formulated and administered with a dose volume not exceeding 1 ml/100 g of mice body weight. Initially, mice were critically observed at different time intervals, such as 15, 30 min, 1, 2, 4, 24, 48, and 72 hr, which was continued for 14 days. In the acute toxicity

study, they were observed for any clinical or behavioral changes and mortality to help determine the nonlethal dose on completion of this study.

3.12.1 | Memory model studies

Gift samples for the standard drugs piracetam and toxicant (scopolamine HBr) were procured from Abbott Healthcare Pvt. Ltd. and Cipla Pvt. Ltd respectively.

3.12.2 | Groups

The Swiss albino mice considered for both the model studies were divided into six groups, each with six animals (three male and three females per group):

Group 1: Control group (untreated)
Group 2: Toxicant group (scopolamine 0.4 mg/kg, i.p.)
Group 3: Standard treatment group (piracetam 200 mg/kg, p.o.)
Group 4: Analogue **11** at dose level one (50 mg/kg, p.o.)
Group 5: Analogue **11** at dose level two (100 mg/kg, p.o.)
Group 6: Analogue **14** at dose level one (50 mg/kg, p.o.)

3.12.3 | Elevated plus maze model

Animals in all groups were subjected to five trials at intervals of 10 min to establish TL on the EPM. Then, all groups, except toxicant, were administered vehicle/standard/test drug for eight consecutive days. On the eighth day, an hour after administration of the last dose, toxicant (scopolamine HBr) was injected to all groups except the vehicle control. After 45 min, the animals were subjected to a training session of 3 min, in which they were individually placed at the end of one open arm facing away from the central platform, and TL in s was calculated from the time the mice moved from an open arm to any enclosed arms. The central platform and the time animals took to move from an open arm to either of the enclosed arms is the TL. On the ninth day, that is, after 24 hr, retention of this learning task was noted in terms of TL.[44]

3.12.4 | Passive avoidance test

Similar to the EPM study, SDL in seconds was estimated using Cook's pole apparatus by the passive avoidance test. In the 3-min training session, animal's latency to step down from the platform on the grid was observed. On stepping down on the grid with all the four paws, for 15 s, they were instantly given electric shocks (1 Hz, 0.5 s, 45 V DC) until they climbed back. On the eighth day after administration of toxicant, the training session was implemented, and after 24 hr, that is, on the ninth day, SDL was recorded to assess memory retention of the learned activity.[45]

4 | CONCLUSIONS

The docking results of benzimidazole analogues depict interactions with BACE1 active site residues. As pointed out earlier, BACE1 enzyme has a pivotal role in AD pathogenesis. All the analogues in the series exhibited drug-like properties. Some analogues exhibited better IC_{50} values in the *in vitro* LPO assay. Thus, it can be envisaged that analogues **11** and **14**, which interact with the catalytic aspartate dyad and exhibit better antioxidant activity, help to retain memory in mice and can be considered potential leads for further optimization and development of more promising analogues with dual role of BACE1 inhibition and neuroprotection.

ACKNOWLEDGMENTS

We acknowledge the University of Mumbai for sanction of Minor Research Project Grant (Research Project No.: 509, Sanction letter No.: APD/ICD/2018-19/593 dated March 16, 2019).

ORCID

Archana S. Gurjar https://orcid.org/0000-0002-3352-3567

REFERENCES

[1] B. M. Gupta, A. Bala, *Ann. Neurosci.* **2013**, *20*(2), 71.
[2] R. Anand, K. D. Gill, A. A. Mahdi, *Neuropharmacology* **2014**, *76*, 27.
[3] C. P. Ferri, M. Prince, C. Brayne, H. Brodaty, L. Fratiglioni, M. Ganguli, K. Hall, K. Hasegawa, H. Hendrie, Y. Huang, A. Jorm, C. Mathers, P. R. Menezes, E. Rimmer, M. Scazufca, Alzheimer's Disease International, *Lancet (London, England)* **2005**, *366*, 2112.
[4] A. Kumar, A. Singh, Ekavali, *Pharmacol. Rep.* **2015**, *67*(2), 195.
[5] R. Macleod, R. T. Cameron, *Future Sci. OA* **2015**, *1*(3), 1.
[6] B. De Strooper, R. Vassar, T. Golde, *Nat. Rev. Neurol.* **2010**, *6*, 99.
[7] T. A. Dineen, M. M. Weiss, T. Williamson, P. Acton, S. Babu-Khan, M. D. Bartberger, J. Brown, K. Chen, Y. Cheng, M. Citron, M. D. Croghan, R. T. Dunn II., J. Esmay, R. F. Graceffa, S. S. Harried, D. Hickman, S. A. Hitchcock, D. B. Horne, H. Huang, R. Imbeah-Ampiah, T. Judd, M. R. Kaller, C. R. Kreiman, D. S. la, V. Li, P. Lopez, S. Louie, H. Monenschein, T. T. Nguyen, L. D. Pennington, T. San Miguel, E. A. Sickmier, H. M. Vargas, R. C. Wahl, P. H. Wen, D. A. Whittington, S. Wood, Q. Xue, B. H. Yang, V. F. Patel, W. Zhong, *J. Med. Chem.* **2012**, *55*, 9025.
[8] A. Cavalli, M. L. Bolognesi, A. Minarini, M. Rosini, V. Tumiatti, M. Recanatini, C. Melchiorre, *J. Med. Chem.* **2008**, *51*(3), 347.

[9] D. Kumar, A. Ganeshpurkar, D. Kumar, G. Modi, S. K. Gupta, S. K. Singh, *Eur. J. Med. Chem.* **2018**, *148*, 436.
[10] S. H. Omara, C. J. Scotta, A. S. Hamlinc, H. K. Obieda, *Fitoterapia* **2018**, *128*, 118.
[11] S. Azimi, A. Zonouzi, O. Firuzi, A. Iraji, M. Saeedi, M. Mahdavi, N. Edraki, *Eur. J. Med. Chem.* **2017**, *138*, 729.
[12] R. J. Lin, T. R. Jinn, S. Jang, F. D. Mai, F. Y. Li, *J. Chin. Chem. Soc.* **2013**, *60*(7), 891.
[13] L. J. Ming, *J. Chin. Chem. Soc.* **2010**, *57*(3A), 285.
[14] C. Shen, Y. Chen, H. Liu, K. Zhang, T. Zhang, A. Lin, N. Jing, *J. Biol. Chem.* **2008**, *283*, 17721.
[15] D. Allan Butterfield, A. Castegna, C. M. Lauderback, J. Drake, *Neurobiol. Aging* **2002**, *23*(5), 655.
[16] A. Kamil, S. Akhtar, S. Jahan, A. Karim, K. Rafiq, S. Hassan, *Int. J. Sci. Eng. Res.* **2013**, *4*, 1674.
[17] M. S. Malamas, J. Erdei, I. Gunawan, K. Barnes, M. Johnson, Y. Hui, J. Turner, Y. Hu, E. Wagner, K. Fan, A. Olland, J. Bard, A. J. Robichaud, *J. Med. Chem.* **2009**, *52*, 6314.
[18] Y. Gravenfors, J. Viklund, J. Blid, T. Ginman, S. Karlström, J. Kihlström, K. Kolmodin, J. Lindström, S. von Berg, F. von Kieseritzky, K. Bogar, C. Slivo, B. M. Swahn, L. L. Olsson, P. Johansson, S. Eketjäll, J. Fälting, F. Jeppsson, K. Strömberg, J. Janson, F. Rahm, *J. Med. Chem.* **2012**, *55*, 9297.
[19] S. Rajasekaran, G. Rao, A. Chatterjee, *Int. J. Drug Dev. Res.* **2012**, *4*(3), 324.
[20] R. Trivedi, S. K. De, R. A. Gibbs, *J. Mol. Catal. A Chem.* **2006**, *245*(1–2), 8.
[21] S. Lin, L. Yang, *Tetrahedron Lett.* **2005**, *46*, 4315.
[22] M. A. Chari, D. Shobha, S. Malayalama, *Int. J. Org. Chem.* **2013**, *3*(December), 243.
[23] D. Kathirvelan, P. Yuvaraj, K. Babu, A. S. Nagarajan, R. Reddy, *Indian J. Chem.* **2013**, *52*(August), 1152.
[24] P. Ghosh, R. Subba, *Tetrahedron Lett.* **2015**, *56*, 1.
[25] K. Bahrami, M. M. Khodaei, I. Kavianinia, *Synthesis (Stuttg)* **2007**, *4*, 547.
[26] Z. Karimi-Jaberi, M. Amiri, *E-J. Chem.* **2012**, *9*(1), 167.
[27] Y. Venkateswarlu, S. R. Kumar, P. Leelavathi, *Org. Med. Chem. Lett.* **2013**, *3*(1), 7.
[28] R. Srinivasulu, K. Ravi Kumar, P. Veera Venkata Satyanarayana, *Green Sustain. Chem.* **2014**, *4*, 33.
[29] D. Kesselring, K. Maurer, K. D. Moeller, *J. Am. Chem. Soc.* **2008**, *130*, 11290.
[30] L. M. Munter, H. Sieg, T. Bethge, F. Liebsch, F. S. Bierkandt, M. Schleeger, H. J. Bittner, J. Heberle, N. Jakubowski, P. W. Hildebrand, G. Multhaup, *J. Am. Chem. Soc.* **2013**, *135*, 19354.
[31] L. Hong, R. T. Turner, G. Koelsch, D. Shin, A. K. Ghosh, J. Tang, *J. Biochem.* **2002**, *41*, 10963.
[32] M. A. Abdelsalam, O. M. AboulWafa, E.-S. A. M. Badawey, M. S. El-Shoukrofy, M. M. El-Miligy, N. Gouda, M. M. Elaasser, *Future Med. Chem.* **2018**, *10*, 1159.
[33] A. Boobis, U. Gundert-Remy, P. Kremers, P. Macheras, O. Pelkonen, *Eur. J. Pharm. Sci.* **2002**, *17*(4), 183.
[34] P. S. Kalsi, *Spectroscopy of Organic Compounds*, 6th ed., New Delhi, India: New Age International Publications, p. 286, **2004**.
[35] *Sybyl Version 8.1.1*, Tripos International, St. Louis, MO, **2010**.
[36] *GOLD Version 5.2.2*, CCDC Ltd., England: UK, 2014.
[37] A. S. Gurjar, V. Andrisano, A. D. Simone, V. S. Velingkar, *Bioorg. Chem.* **2014**, *57*, 90.
[38] Suite, Small-Molecule Drug Discovery, *QikProp, Version 3.3, User Manual, Schrödinger*, LLC, New York, NY **2013**, p. 2013.
[39] S. Furniss Brian, J. Hannaford Antony, W. G. Smith peter, *T. A. R. Vogel's Textbook of Practical Organic Chemistry*, 5th ed., London, UK: Longman Group UK Limited, **1989**.
[40] N. Kumar, P. Sharma, A. Pareek, A. Prasad, *Int. J. Chem. Pharm. Sci.* **2013**, *4*(1), 12.
[41] M. N. Alam, N. J. Bristi, M. Rafiquzzaman, *Saudi Pharm. J.* **2013**, *21*(2), 143.
[42] A. V. Smirnov, A. F. Kucheryavenko, A. A. Spasov, *Bull. Exp. Biol. Med.* **2014**, *157*(5), 580.
[43] B. Mathew, J. Suresh, S. Anbazhagan, *J. Saudi Chem. Soc.* **2016**, *20*, S132.
[44] J. Itoh, T. Nabeshima, T. Kameyama, *Psychopharmacology (Berl)* **1990**, *101*, 27.
[45] M. R. Zarrindast, M. Bananej, A. Khalilzadeh, S. Fazli-Tabaei, A. Haeri-Rohani, A. Rezayof, *Neurobiol. Learn. Mem.* **2006**, *86*(3), 286.

SUPPORTING INFORMATION

Additional supporting information may be found online in the Supporting Information section at the end of this article.

How to cite this article: Gurjar AS, Solanki VS, Meshram AR, Vishwakarma SS. Exploring beta amyloid cleavage enzyme-1 inhibition and neuroprotective role of benzimidazole analogues as anti-alzheimer agents. *J Chin Chem Soc*. 2019;1–10. https://doi.org/10.1002/jccs.201900200